

Bose-Hubbard model on a kagome lattice with sextic ring-exchange terms

Valéry G. Rousseau, Ka-Ming Tam, Mark Jarrell, and Juana Moreno

Department of Physics & Astronomy and Center for Computation & Technology, Louisiana State University, Baton Rouge, Louisiana 70803, USA

(Received 14 June 2012; revised manuscript received 16 February 2013; published 27 February 2013)

High-order ring-exchange interactions are crucial for the study of quantum fluctuations on many highly frustrated systems. A versatile and efficient quantum Monte Carlo method, which can handle finite and essentially zero temperature and canonical and grand-canonical ensembles, has long been sought. In this paper, we present an exact quantum Monte Carlo study of a model of hard-core bosons with sixth-order ring-exchange interactions on a two-dimensional kagome lattice. By using the *stochastic Green function* algorithm with *global space-time update*, we show that the system becomes unstable in the limit of large ring-exchange interactions. It undergoes a phase separation at all fillings, except at $\frac{1}{3}$ and $\frac{2}{3}$ fillings for which the superfluid density vanishes and an unusual mixed valence bond and charge density ordered solid is formed. This explains the universal features seen in previous studies on various different models, such as the transverse-field Ising models, on a kagome lattice near the classical limit.

DOI: [10.1103/PhysRevB.87.075146](https://doi.org/10.1103/PhysRevB.87.075146)

PACS number(s): 75.10.Kt, 02.70.Uu, 05.30.Jp, 75.10.Jm

Interest in ring-exchange interactions in quantum many-body systems has a long history originating from the study of quantum solids, a typical example being solid helium-3.^{1,2} Recently, the study of ring-exchange interactions has resurged with boson and spin models.³⁻⁸ In particular, multiple particle exchange has been suggested as a possible candidate to induce a normal “Bose metal” or “Bose liquid” phase at zero temperature, in which there are no broken symmetries associated with superfluidity or charge density wave phases.⁸⁻¹¹ Studies on a square lattice with four-site ring-exchange plaquettes suggest that ordered phases always dominate.⁴⁻⁷ However, these results still leave the possibility that a Bose liquid or spin-liquid phase may exist in certain frustrated lattices.^{3,12}

Here, we explore a frustrated kagome lattice built from corner-sharing triangles in two dimensions. The most important characteristic of highly frustrated quantum systems is their ground-state degeneracy in the classical limit.^{13,14} In such systems, the classical ground-state manifold, which is given by the least frustrated Ising spin configurations, results in local constraints in each unit. One of the prominent problems in frustrated quantum magnetism is whether quantum fluctuations partially alleviate the classical ground-state degeneracy via the order-by-disorder mechanism or by forming a quantum spin liquid driven by quantum fluctuations.¹⁴⁻¹⁶ A natural route to study this problem is to construct an effective theory for the low-energy quantum fluctuations which is confined to the Hilbert space of the degenerate classical ground-state manifold. From the strong-coupling perturbation theory, the leading term for the quantum fluctuations involves multiple-spin loop flips which form the ring-exchange term. For kagome and pyrochlore lattices, the smallest ring-exchange term appears at the sixth order.^{9,11,17} Therefore, the study of quantum fluctuations on some of the most important highly frustrated lattices naturally involves effective models with multiple-spin ring exchange.

Recently, those ring-exchange models have been formulated in terms of gauge theories.^{9,10,18} The gauge theory formulation is essentially the manifestation of the constraint for the projected Hilbert space within the classical degenerate manifold, and the effective gauge theory is, in turn, studied

by a duality mapping. Various phases have been proposed for different models based on this type of calculation.

It is extremely important to have a systematic unbiased numerical method to test the various proposals for exotic ordered valence bond and disordered spin-liquid phases. However, numerical studies on those models have proved to be rather difficult. There are some recent studies using the world-line and the stochastic series expansion algorithms with loop-update schemes on four-site ring-exchange models.⁴⁻⁷ For these models, ring-exchange interactions are described by a term that performs a correlated hopping of two particles in opposite directions, with no contribution to the winding. Thus, one can expect the superfluidity to be destroyed when this term is dominant. However, instead of the proposed Bose liquid phase, these exact studies have found charge density waves, valence bond solids, or phase separation.

The model we consider in this work consists of hard-core bosons on a two-dimensional kagome lattice (Fig. 1). The underlying Bravais lattice is spanned by the basis vectors (\vec{a}_1, \vec{a}_2) with lengths chosen as unity, and the kagome lattice is obtained by duplicating a set of three sites $S_1(\frac{1}{2}, 0)$, $S_2(0, \frac{1}{2})$, $S_3(\frac{1}{2}, \frac{1}{2})$ (gray symbols). The reciprocal lattice is spanned by the vectors (\vec{b}_1, \vec{b}_2) , each with length $4\pi/\sqrt{3}$.

The Hamiltonian takes the form (we use periodic boundary conditions)

$$\hat{\mathcal{H}} = -t \sum_{\langle i,j \rangle} (a_i^\dagger a_j + \text{H.c.}) - K \sum_{\bigcirc} (a_1^\dagger a_3^\dagger a_5^\dagger a_6 a_4 a_2 + \text{H.c.}), \quad (1)$$

where a_i^\dagger and a_i are the creation and annihilation operators of a hard-core boson on site i . These operators satisfy fermionic anticommutation rules when acting on the same site, $a_i^2 = 0$, $a_i^{\dagger 2} = 0$, $\{a_i, a_i^\dagger\} = 1$, and bosonic commutation rules when acting on different sites, $[a_i, a_j] = 0$, $[a_i^\dagger, a_j^\dagger] = 0$, $[a_i, a_j^\dagger] = 0$. The usual kinetic term allows the particles to hop between near-neighboring sites i and j . A sextic ring-exchange term allows three particles to perform a correlated hopping within the same hexagon, with the \sum_{\bigcirc} over all hexagons. We study the model as a function of filling factor and K/t .

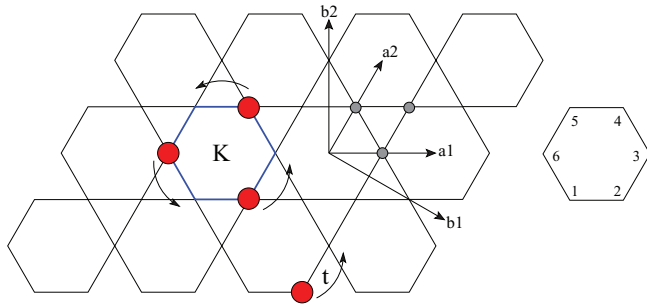


FIG. 1. (Color online) The kagome lattice and the effect of the different terms in the Hamiltonian. Each site is shared by two hexagons, so the total number of sites is three times the number of hexagons (for a periodic lattice). The usual kinetic term t allows the particles to hop between near-neighboring sites. The ring-exchange term K performs a correlated hopping of three particles within the same hexagon. This process is possible only if the hexagon contains exactly three non-near-neighboring particles. The figure also shows our convention for the labels of the sites of a given hexagon.

This model can be mapped to the U(1) lattice gauge theory with a softened hard-core constraint, which plays a crucial role in the study of quantum fluctuations in some highly frustrated models.^{9,11} Notably, similar models can possibly be realized in optical lattices with dipolar bosons.¹⁹ Since the sextic ring-exchange term couples six different sites at a time, an analytical treatment of the Hamiltonian (1) is rather complicated.^{9,11} On the other hand, most current quantum Monte Carlo (QMC) methods used on a square lattice⁴⁻⁷ need to decompose the Hamiltonian as a sum of two-site coupling terms, which is not possible in our case. These methods need such a decomposition because they use a *loop update* that consists of building a closed path in space and imaginary time, and raising or lowering the occupation number of the sites that are visited. By construction, these loops can update only one or two sites at a time, and are therefore suitable only for one- or two-site coupling terms. In brief, the treatment of fourth-order ring-exchange terms in previous studies required some special developments^{4,7} that are not easy to generalize to sixth or higher order.

However, the *stochastic Green function* (SGF) algorithm^{20,21} with global space-time update²² does not make use of such loop updates, instead, it performs a direct sampling of the partition function by distributing Hamiltonian terms randomly in space and imaginary time. No particular decomposition of the Hamiltonian is required. Therefore, the update procedure is totally independent of the structure of the Hamiltonian, and can be applied to any n -site coupling term with efficiency. In this work, we use the SGF algorithm and perform simulations of systems with sizes up to 18×18 hexagons (972 sites).

While the SGF algorithm is designed to work in the canonical ensemble (CE), an extension²² allows us to simulate the grand-canonical ensemble (GCE). In the following, we take advantage of this flexibility. We find it convenient to use the GCE for studying the stability of the system. However, it is much easier to use the CE on parameter regions where the system is stable only at specific densities. This is, to the best of our knowledge, an unbiased QMC method that allows the

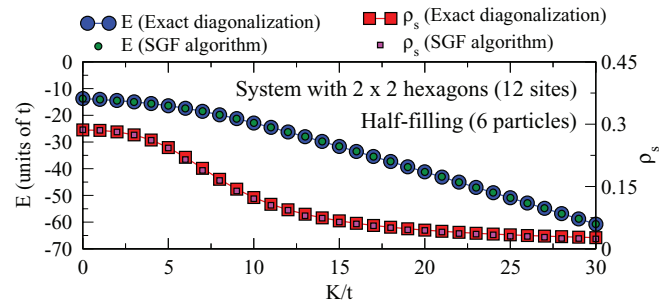


FIG. 2. (Color online) Comparison between an exact diagonalization and the SGF algorithm for the energy E and the superfluid density ρ_s .

simulation of sixth-order coupling terms in both the CE and GCE at both finite and essentially zero temperatures. For the GCE, we add the usual term $-\mu\hat{N}$ to the Hamiltonian (1), where μ is the chemical potential and \hat{N} is the total particle-number operator. In the CE, μ is not a control parameter, but it is measured at zero temperature as $\mu(N) = E(N+1) - E(N)$, where $E = \langle \hat{H} \rangle$ and N is the controlled number of particles.

In the following, we show that the model contains valence bond solids at densities $\rho = \frac{1}{3}$ and $\frac{2}{3}$ when the ring-exchange term is dominant. For our study, we will consider the superfluid density

$$\rho_s = \frac{\langle \hat{W}_1^2 + \hat{W}_2^2 \rangle}{4t\beta}, \quad (2)$$

where β is the inverse temperature and \hat{W}_1 and \hat{W}_2 are the winding numbers measured in the two directions \vec{a}_1 and \vec{a}_2 . We also consider the structure factor $S(\vec{k}) = \langle |\tilde{n}(\vec{k})|^2 \rangle$, with

$$\tilde{n}(\vec{k}) = \frac{1}{3L^2} \sum_p (\hat{n}_p - \rho) e^{-i\vec{k}\cdot\vec{r}_p}, \quad (3)$$

where L is the linear system size (counting hexagons), ρ is the density, $\hat{n}_p = a_p^\dagger a_p$ is the number operator on site p , and \vec{r}_p is the position of site p . Note that the subtraction of ρ in (3) is meant to get rid of the lattice Bragg peaks. In order to study the ground-state properties, we systematically use the inverse temperature $\beta = 2L/t$.

We start by illustrating in Fig. 2 the exactness of the SGF results by comparing them with an exact diagonalization on a lattice with 2×2 hexagons (12 sites) and six particles. The figure shows an excellent agreement for the energy E and the superfluid density ρ_s .

It is useful to analyze first the stability of the system. This is easily done by looking at the total density ρ as a function of the chemical potential μ . The slope of this function is proportional to the compressibility of the system, so an instability of the system results either in a negative slope in the CE or a discontinuity of the total density in the GCE. We first discuss the small- K region, and search for any phase transition as we increase the value of K . Figure 3 shows results for $K = 5t$ and a system with 4×4 hexagons (48 sites) in the CE and 12×12 hexagons (432 sites) in the GCE. The agreement between the two curves reveals that finite-size effects are sufficiently small to ensure the equivalence of the two ensembles. For this

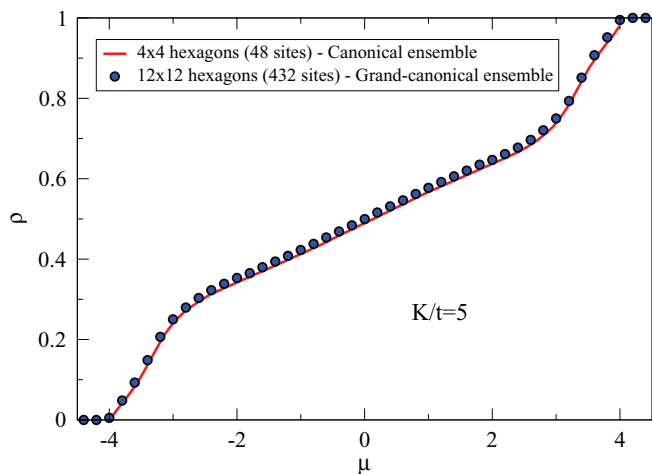


FIG. 3. (Color online) The total density ρ as a function of the chemical potential μ for $K = 5t$. Results for a lattice with 4×4 hexagons in the canonical ensemble and 12×12 hexagons in the grand-canonical ensemble are shown. The agreement between the two curves reveals that finite-size effects are sufficiently small to ensure the equivalence of the two ensembles.

strength of the ring-exchange interactions, the slope of the curve remains positive and finite at all fillings, so there is no instability.

The situation changes as K increases. Figure 4 shows the total energy E as a function of the density ρ in the CE for $K/t = 10$ and 25 . We show only data for $\rho \leq \frac{1}{2}$ since the data for $\rho > \frac{1}{2}$ can be deduced by particle-hole symmetry. The cyan dotted line serves as a guide to indicate that the curvature of the $K/t = 10$ curve is positive for $\rho \in [\frac{1}{3}; \frac{2}{3}]$, while the orange dotted lines emphasize regions with negative curvatures. Systems for which the energy has a negative second derivative with respect to the density are thermodynamically unstable and undergo a phase separation. We also note the presence of a kink at $\rho = \frac{1}{3}$ for both curves, which indicates a gapped phase. We conclude that for $K/t = 10$, the system

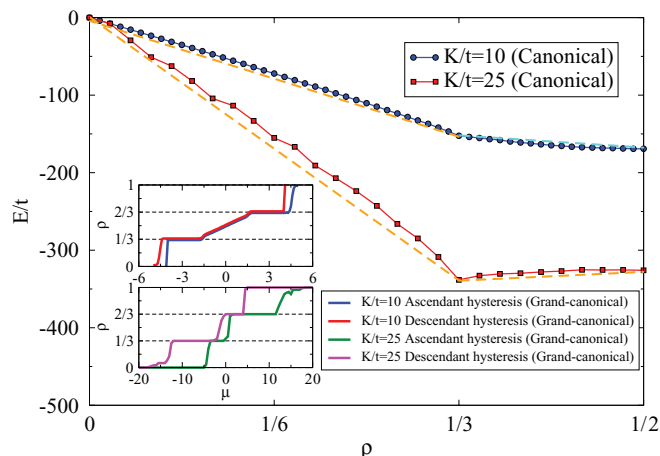


FIG. 4. (Color online) The energy as a function of the density for $K/t = 10$ and 25 in the CE. The insets show for comparison the density as a function of the chemical potential in the GCE, with a numerical hysteresis. See text for details.

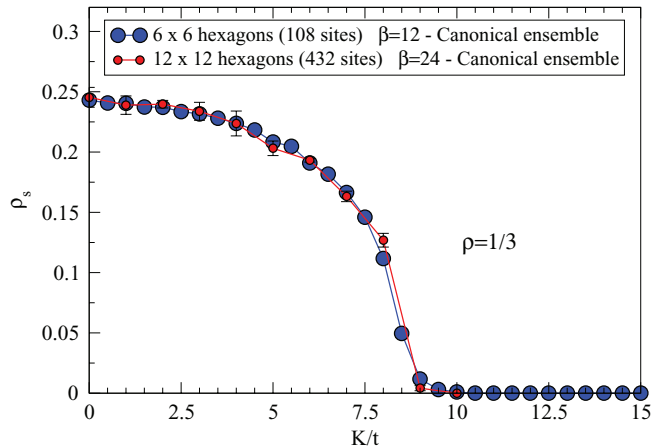


FIG. 5. (Color online) The superfluid density ρ_s as a function of K/t for $\rho = \frac{1}{3}$. The superfluid density is completely destroyed at the critical value $K_c \approx 9t$.

is compressible for $\rho \in]\frac{1}{3}; \frac{2}{3}[$ and in a solid phase for $\rho = \frac{1}{3}$ and $\frac{2}{3}$, while it is unstable for all other densities. For $K/t = 25$, the system is unstable for all densities, except for $\rho = \frac{1}{3}$ and $\frac{2}{3}$ for which the phase is solid. The insets correspond to GCE results that are in agreement and which, in addition to showing “jumps” over the “forbidden” densities, show the existence of a “numerical hysteresis,” depending on if the initial state is empty (ascendant hysteresis) or full (descendant hysteresis). This phenomenon is observed in many Monte Carlo studies,^{23,24} including the four-site ring-exchange model.⁶ For these parameters, the grand-canonical algorithm is no longer able to sample all contributing states, which is an indication that the system undergoes a spontaneous symmetry breaking in the thermodynamic limit. This also supports the importance of the ability of the SGF algorithm to work in the canonical ensemble.

Since only the fillings $\rho = \frac{1}{3}$ and $\frac{2}{3}$ are stable in the large- K limit, it is convenient to analyze how the superfluid density ρ_s is destroyed as a function of K/t by working in the CE. We show in Fig. 5 results for $\rho = \frac{1}{3}$ only, the case with $\rho = \frac{2}{3}$ being identical because of the particle-hole symmetry. There exists a critical value of the ring-exchange interaction $K_c \approx 9t$ where the superfluid density vanishes. We show results for 6×6 hexagons (108 sites) and 12×12 hexagons (432 sites) to illustrate that finite-size effects are small.

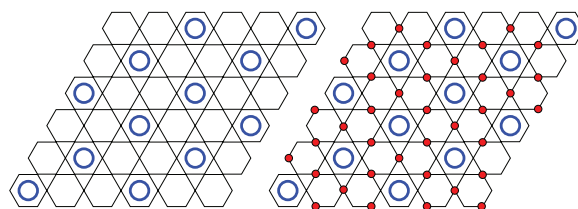


FIG. 6. (Color online) Two possible ordering patterns for $\rho = \frac{1}{3}$ (left) and $\rho = \frac{2}{3}$ (right). The circles inside the hexagons represent three resonating particles. The red dots represent localized particles. We note that both orderings have threefold degeneracy. These two uniform ordering patterns are only formed for $\rho = \frac{1}{3}$ and $\frac{2}{3}$. Other fillings are unstable towards phase separation.

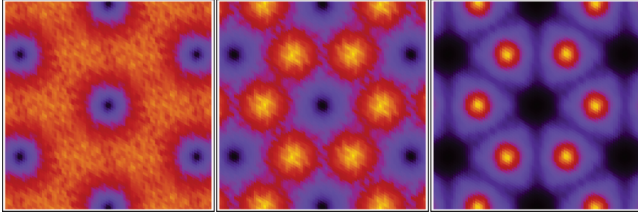


FIG. 7. (Color online) The structure factor $S(\vec{k})$ for 18×18 hexagons (972 sites), $\rho = \frac{1}{3}$ and $K = 0$ (left panel), $K = 5t$ (middle panel), and $K = 15t$ (right panel). The black regions correspond to the locations of the lattice Bragg peaks. As K increases, peaks with maximum intensity develop at $k = \frac{2}{3}\vec{b}_1 + \frac{1}{3}\vec{b}_2$ and symmetry-related momenta.

For $t \gg K$, the model is in the free hard-core limit, thus the superfluid phase prevails against solid or valence bond ordering. In the opposite $t \ll K$ limit, we expect the ground state to be formed by configurations that maximize the number of resonating hexagons. Because a resonance can occur only if the hexagon contains exactly three non-first-neighboring particles, it is not possible to have two resonating neighboring hexagons at first order in K . This suggests that a phase with a maximum number of resonating hexagons can be formed at $\rho = \frac{1}{3}$ by having all resonating hexagons surrounded by empty hexagons (Fig. 6 left), or at $\rho = \frac{2}{3}$ by having all resonating hexagons surrounded by hexagons that contain three localized particles on the vertices of the triangles that are not shared with the resonating hexagons (Fig. 6 right). These phases can be understood as a form of valence bond solid in which each valence bond now involves six sites, in contrast with the usual two-site singlets. We note that the phase has been suggested in kagome lattice on other models, such as the transverse-field Ising model.^{11,25}

This scenario is confirmed by looking at the structure factor. Figure 7 shows $S(\vec{k})$ for 18×18 hexagons (972 sites) with

$\rho = \frac{1}{3}$, $K = 0$, $K = 5t$, and $K = 15t$. For $K = 0$ (left panel), only lattice Bragg peaks arise and correspond to the minima of the intensity (black and blue). For $K = 5t$ (middle panel), high-intensity regions (red and yellow) appear in the center of triangles formed by the Bragg peaks. In the insulating phase $K = 15t$ (right panel), the high-intensity regions become localized at $k_{\max} = (\frac{2}{3}, \frac{1}{3})$ in the (\vec{b}_1, \vec{b}_2) basis (and symmetry-related momenta), and form a honeycomb lattice. Since \vec{k}_{\max} is parallel to \vec{a}_1 and $||\vec{k}_{\max}|| = \frac{4\pi}{3}$, the insulating phase has features that appear with a spatial frequency of $\frac{2}{3}$ in the \vec{a}_1 direction, in agreement with Fig. 6.

To conclude, we study hard-core bosons on a kagome lattice with a sextic ring-exchange term using the stochastic Green function algorithm.²⁰⁻²² We find that the system becomes unstable towards phase separation as the ring-exchange interaction increases, except for densities $\rho = \frac{1}{3}$ and $\frac{2}{3}$ where the superfluid is destroyed. Here, we observe an unusual valence bond solid phase with resonances involving six sites simultaneously. The hysteresis obtained in the quantum Monte Carlo indicates that the phase transition between the superfluid and the valence bond solid at $\rho = \frac{1}{3}$ and $\frac{2}{3}$ is first order. Models with higher-order ring-exchange played an important role in the search of spin-liquid phases due to their relation with the gauge theory deconfined phase. This work showcases the power of the stochastic Green function algorithm to study models with higher-order ring-exchange interactions which have hitherto been very challenging for other Monte Carlo methods.

We thank C. Duran for careful reading of the manuscript. This work is supported by DOE SciDAC Grant No. DE-FC02-06ER25792 (K.M.T. and M.J.) and by NSF OISE-0952300 (V.G.R. and J.M.). This work used the Extreme Science and Engineering Discovery Environment (XSEDE), which is supported by National Science Foundation Grant No. DMR100007.

¹D. J. Thouless, *Proc. Phys. Soc., London* **86**, 893 (1965).

²C. Herring, *Rev. Mod. Phys.* **34**, 631 (1962).

³L. Balents, M. P. A. Fisher, and S. M. Girvin, *Phys. Rev. B* **65**, 224412 (2002).

⁴A. W. Sandvik, S. Daul, R. R. P. Singh, and D. J. Scalapino, *Phys. Rev. Lett.* **89**, 247201 (2002).

⁵V. G. Rousseau, G. G. Batrouni, and R. T. Scalettar, *Phys. Rev. Lett.* **93**, 110404 (2004).

⁶R. G. Melko, A. W. Sandvik, and D. J. Scalapino, *Phys. Rev. B* **69**, 100408(R) (2004).

⁷V. G. Rousseau, R. T. Scalettar, and G. G. Batrouni, *Phys. Rev. B* **72**, 054524 (2005).

⁸A. Paramekanti, L. Balents, and M. P. A. Fisher, *Phys. Rev. B* **66**, 054526 (2002).

⁹M. Hermele, M. P. A. Fisher, and L. Balents, *Phys. Rev. B* **69**, 064404 (2004).

¹⁰P. Nikolic and T. Senthil, *Phys. Rev. B* **68**, 214415 (2003).

¹¹P. Nikolic and T. Senthil, *Phys. Rev. B* **71**, 024401 (2005).

¹²L. Dang, S. Inglis, and R. G. Melko, *Phys. Rev. B* **84**, 132409 (2011).

¹³J. Villain, *Z. Phys. B: Condens. Matter Quanta* **33**, 31 (1979).

¹⁴*Frustrated Spin Systems*, edited by H. T. Diep (World Scientific, Singapore, 2005).

¹⁵J. Villain, R. Bidaux, J.-P. Carton, and R. Conte, *J. Phys. (France)* **41**, 1263 (1980).

¹⁶E. F. Shender, *Sov. Phys.-JETP* **56**, 178 (1982).

¹⁷N. Shannon, O. Sikora, F. Pollmann, K. Penc, and P. Fulde, *Phys. Rev. Lett.* **108**, 067204 (2012).

¹⁸A. H. Castro Neto, P. Pujol, and E. Fradkin, *Phys. Rev. B* **74**, 024302 (2006).

¹⁹S. Tewari, V. W. Scarola, T. Senthil, and S. Das Sarma, *Phys. Rev. Lett.* **97**, 200401 (2006).

²⁰V. G. Rousseau, *Phys. Rev. E* **77**, 056705 (2008).

²¹V. G. Rousseau, *Phys. Rev. E* **78**, 056707 (2008).

²²V. G. Rousseau and D. Galanakis, arXiv:1209.0946.

²³K. S. D. Beach and A. W. Sandvik, *Phys. Rev. Lett.* **99**, 047202 (2007).

²⁴F. Hébert, G. G. Batrouni, R. T. Scalettar, G. Schmid, M. Troyer, and A. Dorneich, *Phys. Rev. B* **65**, 014513 (2001).

²⁵H. W. J. Blöte and Y. Deng, *Phys. Rev. E* **66**, 066110 (2002).